

# Reliability verification of mooring components for floating marine energy converters

## Vérification de la fiabilité des composants d'un amarrage de convertisseur d'énergie des vagues

Tessa Gordelier<sup>1</sup>, Lars Johanning, Philipp R. Thies

University of Exeter, UK  
Renewable Energy, Tremough Campus, TR10 9EZ, UK  
Tel<sup>1</sup>. +44 (0)1326 254188  
e-mail<sup>1</sup>: tjc206@exeter.ac.uk

### ABSTRACT

Safety factors are critical to device reliability and are applied during device development to protect against early failures. At each stage of a development a designer may apply their own safety factor in relation to the criticality of the component or subassembly for which they are responsible. This paper seeks to understand how different assessment techniques can assist the design process by refining safety factors, with the aim of reducing device costs and improving economic viability.

To achieve this, a methodology is presented to assess and verify the fatigue performance of mooring components. The paper draws on field data and introduces a combined approach of modelling, service simulation and field tests to validate the reliability of components. A shackle is used as a case study to demonstrate the methodology. Results from finite element analysis (FEA) and accelerated service simulation testing on the Dynamic Marine Component test facility (DMaC) are presented and discussed, including fatigue damage and failures.

FEA is found to accurately predict areas of weakness within a component, however it underestimates component strength due to unrealistic stress concentrations at applied boundary conditions. Static and fatigue tests demonstrate the complex nature of reliability estimation, with static component safety factors of 8.6 being reduced to less than 3.7 under a fatigue loading regime. Service simulation testing is found to be important in refining initial reliability estimations from S-N curves and FEA models. The effect of mean stress on fatigue failure is also found to be significant.

**Key words:** Wave energy, reliability, mooring, fatigue, failures, safety factor.

### I INTRODUCTION

The reliability of mooring systems is crucial for viable commercial installations of floating marine energy converters. The station-keeping must be secure, yet the mooring arrangement must be sufficiently compliant to allow the dynamic motions required for power conversion. High safety factors are a simple solution to improve reliability but are associated with increased equipment and deployment costs. The engineering challenge is to decrease uncertainties in component behaviour prior to deployment. By establishing the evidence that the system will be reliable under the expected operating conditions, excessive design safety factors can be reduced.

Reducing the cost of wave energy is essential for it to become competitive with other forms of energy generation. [1] suggests a cost saving of 50-75% must be achieved by 2025 for wave energy to become a commercial reality. Moorings are a key area for cost reduction, and the potential for cost savings is highlighted in [2], which details moorings as one of three priority components for cost reduction in wave energy converters (WECs). 7% - 10% of the capital costs of a wave farm can be attributed to moorings [1, 2]. In an analysis on potential savings 50%/85% savings on the mooring

---

<sup>1</sup> Corresponding author

system could be achieved by 2020/2050 respectively by efficiency improvements and improved deployments of mooring systems [1].

Safety factors are applied throughout the design process. In mooring systems alone the shackle manufacturer will apply a safety factor of approximately 5, and in addition the mooring designer may apply a further safety factor based on DNV guidance [3]. Within this guidance various safety factors are suggested. Based on Ultimate Limit State (whereby each individual mooring line has adequate strength to withstand extreme environmental conditions), and based upon Consequence Class 1 (a failure is unlikely to lead to unacceptable consequences such as loss of life), a maximum safety factor of 1.7 is suggested. However, when looking at design for fatigue, the minimum safety factor suggested is 5. The increased size of the mooring systems to account for these safety factors can have implications for the design of the WEC body itself, which may require alterations to cope with the increased loads. The accumulation of these safety factors can lead to significant device costs, and this work seeks to understand whether such high safety factors are always necessary.

Further to the potential cost savings, the importance of reliable mooring systems is evident from a brief review of the literature. There are a large number of devices under development [4, 5] and no convergence on one device type. However, the literature indicates a clear progression towards Point Absorber devices. In 2010, [5] details that Point Absorbers account for over 50% of devices currently under development. Point absorbers generate energy by the relative movement of different parts of the device activated by the motion of the waves and are located nearshore or offshore. They have small dimensions relative to the wave front and either float on the wave surface or are submerged just beneath the wave surface [5-8]. Effective mooring systems are therefore crucial to the mode of operation for point absorbers.

There have been numerous reports providing recommendations on key aspects requiring research and development to bring commercial wave energy to a reality. A detailed review of the recommendations from five reports [2, 9-12], issued by various bodies over the period 2002 – 2010, highlights two components listed as a priority area in every report; the power take off system (PTO) and the mooring system. To focus research on a more generic component, the recommendations from these reports were also assessed for commonality across different devices. It was concluded that moorings are a more generic component, as many PTOs will be specific to a device.

The importance of mooring systems is evident from the potential for cost savings and the dominance of the Point Absorber device type. The review of recommendations from five technology reports has further confirmed the importance of mooring systems. The approach suggested in this paper will contribute to the development of reliable and cost effective mooring components, by improved understanding of the application of safety factors in the design process.

## **II APPROACH & METHODOLOGY**

The method presented here proposes a combination of finite element analysis (FEA), accelerated component testing and field deployment of components in order to assess reliability and fatigue behaviour. A case study is presented to develop the approach using a standard component; a steel shackle. A flow chart is detailed in Figure 1 that sets out the key steps of the approach. The sea deployment will not be covered in this paper.

### **II - 1 Field measurement**

The component tests have been informed by extensive field measurements that have been conducted at the South West Mooring Test Facility (SWMTF) [13, 14]. It is located in Falmouth Bay, Cornwall, UK (50°47.5'N 5°2.85'W) and consists of a generic buoy that has been installed with a three-leg catenary hybrid (rope-chain) mooring since March 2010.

The mooring lines have been fitted with tri-axial and in-line load cells to monitor and record the tensile mooring loads during the operation in real sea conditions. The installation site is relatively

sheltered with mean annual wave power levels in the order of 5kW/m in a water depth of 27-32.4m. The peak loads that have been recorded during significant wave heights of  $H_s=3.5\text{m}$  range in the order of 50kN, with the maximum recorded at 53kN.

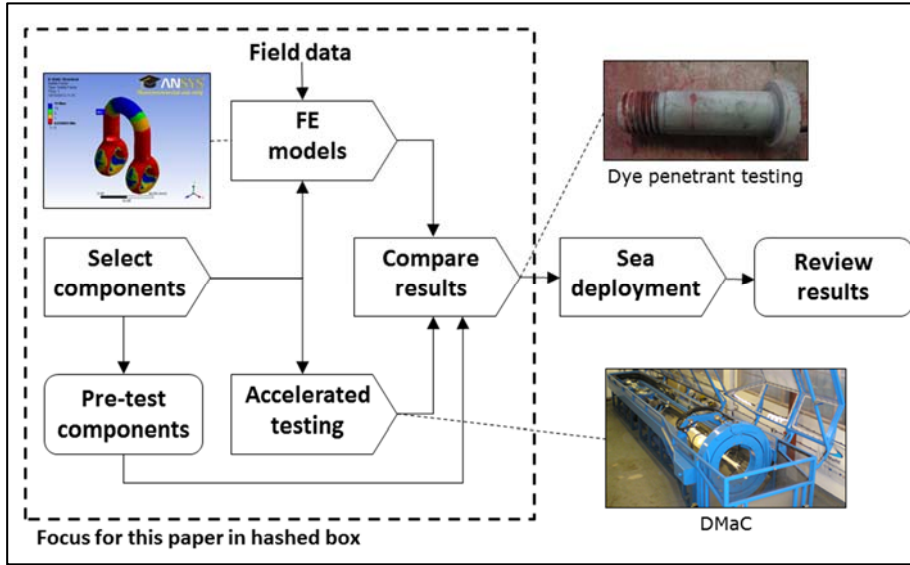


**Figure 1: Simplified process for the methodology highlighting the focus for this paper**

## II - 2 Shackle selection and fatigue considerations

Shackles are generally specified by Safe Working Load (SWL) or Working Load Limit (WLL). This is the maximum load the shackle should be exposed to in use. A Minimum Breaking Load (MBL) is also specified, which is the minimum load required to cause failure. The MBL is related to the WLL by a safety factor (SF):

$$WLL = MBL \times SF \quad (1)$$

The safety factor applied ranges depending on specification but is often 4 to 6.

Field measurements were considered when specifying the shackle, to ensure it would survive extreme loads but remain susceptible to fatigue damage at the SWMTF site. This requires an understanding of the fatigue behaviour of the material. There is limited material data available from shackle suppliers; although the yield strength and the tensile strength are often provided, S-N curves (detailing fatigue response to a given load and cyclical loading regime) remain elusive. Detailed fatigue experiments are beyond the scope of this research and instead approximations will be taken from Det Norske Veritas (DNV) guidance. DNV provide guidance in their offshore standard for position mooring [3] and refer to the use of the B1 S-N curve parameters as detailed in their recommended practice for fatigue design of offshore steel structures [15]. They suggest these curves are appropriate for calculating the fatigue life of long term mooring shackles and are associated with a 97.7% probability of survival. The general equation for the S-N curve is as follows:

$$\log N = \log \bar{a} - m \log \Delta \sigma \quad (2)$$

Where  $N$  is the number of cycles to failure,  $\bar{a}$  is the intercept of the x axis,  $m$  is the negative inverse slope of the S-N curve and  $\Delta \sigma$  is the stress range.

In this set of experiments the DNV S-N curve for shackles in air will be utilised, defined by:

$$\log N = 15.117 - 4 \log \Delta \sigma \quad (3)$$

For  $N \leq 10^7$  cycles

$$\log N = 17.146 - 5 \log \Delta \sigma \quad (4)$$

For  $N > 10^7$  cycles

The following shackle type was specified: B.S. 3032, galvanized steel shackle, working load limit 2.5t (24.5kN), SF 5, minimum breaking load 12.5t (122.6kN), yield strength 890 MPa, tensile strength 1010 MPa.

### **II - 3 Numerical investigation (FEA)**

For the initial FEA modelling an existing CAD model was imported from a manufacturer catalogue [16]. This model was imported to ANSYS FEA software for analysis. The pin and the shackle were analysed individually in static simulations to remove complex interactions in the model for the first iteration of the analysis. Different loading regimes were applied to reflect mooring loads measured at the SWMTF and to review the shackle response to loads at the WLL and MBL of the specified shackle.

Material data applied to the model reflected the data provided by the shackle manufacturer. Although limited, this included figures for yield point, tensile strength and elongation. Design points were created in the model to allow the exploration of the effects of applied load on the stresses created within the shackle, and to gain an understanding of what load is required to induce yield and ultimate failure in the shackle.

Boundary conditions were applied as follows:

Shackle pin - fixed supports applied at either end of the pin, load applied in centre of pin.

Shackle bow - fixed supports applied to the bow of the shackle, load applied to the lower half of the inner shackle eyes.

### **II - 4 Experimental methods**

The experimental procedure was conducted in the Dynamic Marine Component test facility (DMaC) based in Falmouth Docks, Cornwall, UK. This test facility was developed to replicate the loading conditions imposed by sea states, in a controlled environment with detailed monitoring, and with the option of accelerating the testing regime [17]. The DMaC can be operated in either force driven or displacement driven testing regimes, and has the option of conducting tests fully immersed in water.

#### **II - 4 a) Break tests**

The aim of the break tests was to evaluate the shackle behaviour in comparison to the supplier specification and the FE model, and also to define the yield point of the shackle to inform the fatigue tests.

Identical break tests were conducted on two individual shackles. Displacement mode was used to conduct the break tests. A displacement of 0.1m was used; from the FE model this would ensure complete failure of the shackle in one cycle.

#### **II - 4 b) Fatigue tests**

The fatigue tests were intended to 'pre-age' three sets of shackles to differing levels of damage. To keep the complexity of the testing to a minimum it was decided to conduct constant amplitude fatigue tests, as opposed to variable amplitude fatigue tests. Although this is clearly a simplification of a general sea state, there are limitations when quantifying variable amplitude loading and this investigation is not intended to address this.

The level of loading applied was identified from the break tests. This ensured the fatigue ageing occurred in the elastic region of the shackle prior to the yield point. Developing the fatigue loading frequency regime required a compromise between load accuracy and testing time. Following preliminary tests, 2 Hz was specified.

A load driven regime was defined based on the results from the break tests. Pre-tension of 10kN was applied to ensure the samples were taut and load paths were clear, with a maximum of 90kN applied to conduct the fatigue cycles below the yield strength of the shackles.

Three ageing regimes were specified with increasing numbers of cycles. To calculate the accumulated damage over the three regimes, the Palmgren-Miner damage model was applied, as recommended in the guidance [18, 19]. The rule operates cumulatively over a series of different stress amplitudes and works on the basis that if failure occurs at  $N$  cycles for a given stress amplitude, cycling to  $n$  cycles at

the same stress amplitude will cause relative damage  $D$ . The cumulative damage can be summated over  $k$  different stress ranges to give

$$D = \sum_{i=1}^k \frac{n_i}{N_i} \quad (5) \text{ and incorporated into}$$

equation (2) to create  $\sigma_v = \sqrt{\frac{(\sigma_{11}-\sigma_{22})^2+(\sigma_{22}-\sigma_{33})^2+(\sigma_{11}-\sigma_{33})^2+6(\sigma_{12}^2+\sigma_{23}^2+\sigma_{31}^2)}{2}}$

(7) (6):

$$D = \sum_{i=1}^k \frac{n_i}{N_i} \quad (5)$$

$$D = \frac{1}{a} \sum_{i=1}^k n_i (\Delta\sigma_i)^m \quad (6)$$

Dye penetrant testing was selected to identify fatigue crack development in damaged but un-failed specimens. This qualitative method uses dye to identify fatigue crack development not visible to the naked eye. The use of X-ray was also investigated for defect detection but proved less effective.

### III RESULTS

#### III - 1 Numerical investigation (FEA)

Two results will be discussed here that are particularly suitable for summarising the data from the model. Firstly  $\sigma_v$ , the Von-Mises stress (or equivalent stress) which is helpful as it provides a single, equivalent stress for assessment against the yield or ultimate strength of a component. The general

equation for Von-Mises stress is detailed in  $\sigma_v = \sqrt{\frac{(\sigma_{11}-\sigma_{22})^2+(\sigma_{22}-\sigma_{33})^2+(\sigma_{11}-\sigma_{33})^2+6(\sigma_{12}^2+\sigma_{23}^2+\sigma_{31}^2)}{2}}$

(7), and a common simplification (as utilised by ANSYS), which only considers the principal stresses  $i$

$$\sigma_v = \sqrt{\frac{(\sigma_{11}-\sigma_{22})^2+(\sigma_{22}-\sigma_{33})^2+(\sigma_{11}-\sigma_{33})^2+6(\sigma_{12}^2+\sigma_{23}^2+\sigma_{31}^2)}{2}} \quad (7)$$

$$\sigma_v = \sqrt{\frac{(\sigma_{11}-\sigma_{22})^2+(\sigma_{22}-\sigma_{33})^2+(\sigma_{11}-\sigma_{33})^2}{2}} \quad (8)$$

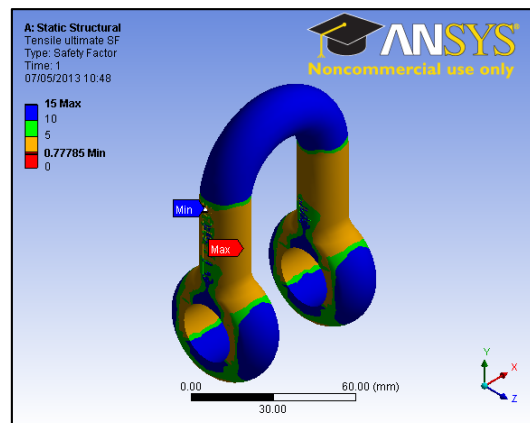
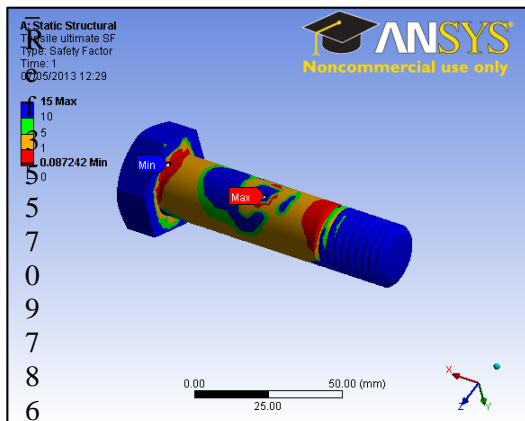
Using the common terminology where  $\sigma_{11}, \sigma_{22}$  and  $\sigma_{33}$  denote principal stresses and  $\sigma_{12}, \sigma_{23}$  and  $\sigma_{31}$  denote shear stresses.

Two

- a) Applied load of 53kN, reflecting the maximum load measured at SWMTF
- b) Applied load of 122.6kN, reflecting the MBL of the shackle.

Maximum

The second metric, particularly informative when considering failures, is the Safety Factor (SF). This provides a figure for the safety factor a component has with regard to yield or ultimate strength (depending which is specified). When  $SF < 1$ , yield or failure has occurred. Contour plots of the ultimate strength safety factor are detailed in Figure 2. The pin shows weaknesses with several areas in red, indicating a  $SF < 1$  and hence failure. The shackle bow on the other hand shows a better response but has some areas of weakness under load b), particularly around the commencement of the bow curvature.



\

M

**Figure 2: Ultimate strength safety factor for pin and bow with load b**

To bring the various results together and detail the VM stress and safety factor over a range of applied loads Figure 3 has been included.

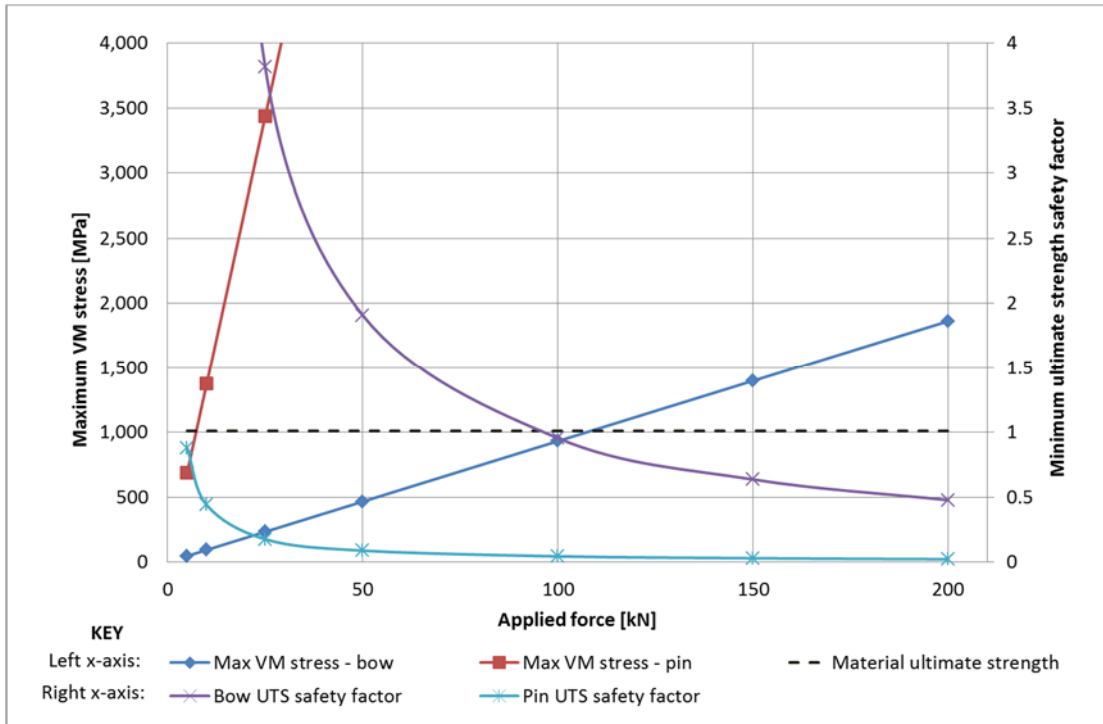


**Figure 3: Maximum VM stress and minimum ultimate tensile strength (UTS) safety factor at different applied loads for bow and pin models**

**III - 2 Experimental results**

**III - 2 a) Break tests**

Two break tests were conducted. Failure loads occurred at 206.5kN and 214.6kN for Break 1 and Break 2 respectively (Figure 4). These are significantly higher than the MBL specified by the manufacturer; the mean recorded break load has a factor of safety of 8.6 on the WLL, and a factor of safety of 1.7 on the MBL.

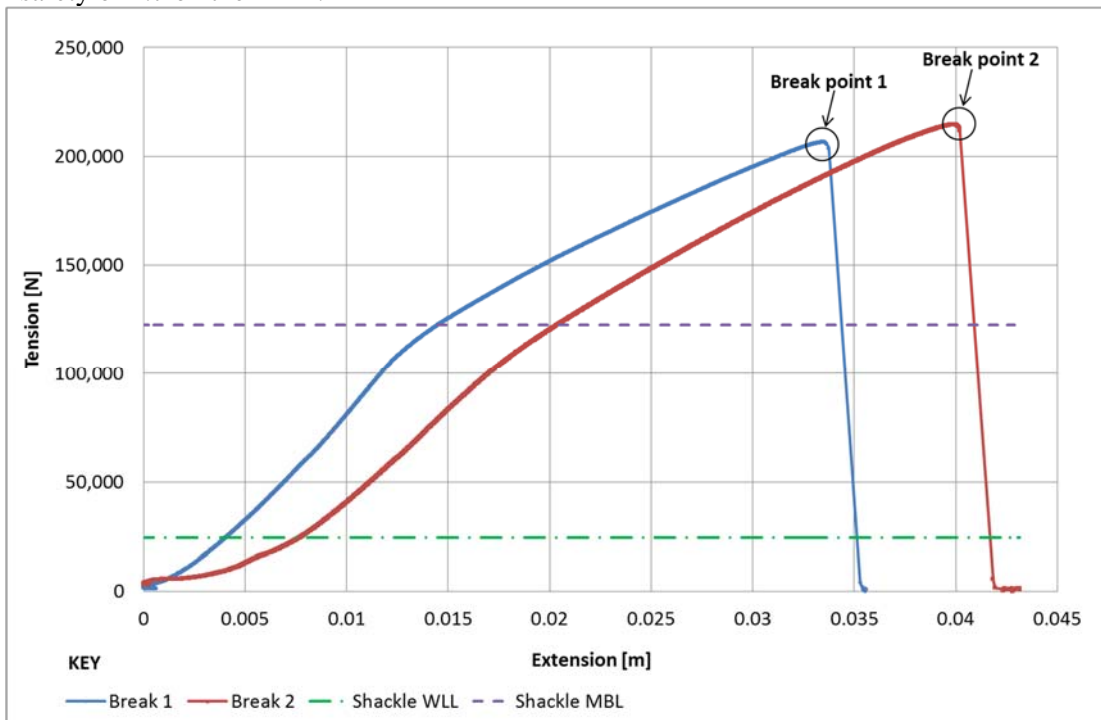


**Figure 4: Break test 1 and 2**

From Figure 4 it is assumed that neither shackle yielded before 100kN; this was used to define the fatigue loading regime. Both failures occurred on the pin at the start of the thread (**Error! Reference source not found.**).



**Figure 5: Shackles from Break Test 1, Break Test 2 and an undamaged shackle for reference**

**III - 2 b) Fatigue tests**

Based

Shackle	Test	Failure	No	Accumulated	Mean
4	Low	No	4,958	0.023	<i>0.127</i>
5	Low	No	4,958	0.023	<i>0.127</i>
6	Med	No	19,386	0.09	<i>0.456</i>
7	Med	No	19,386	0.09	<i>0.456</i>
8	Med	BREAK	19,386	0.09	<i>0.456</i>
9	High	Fatigue	24,344	0.113	<i>0.583</i>
10	High	Fatigue	24,344	0.113	<i>0.583</i>
11	High	BREAK	24,344	0.113	<i>0.583</i>

Table 1 details the fatigue tests, with location of failures and the % damage induced based on the S-N curve discussed in **II - 2** and the Palmgren Miner rule introduced in **II - 4b**. Mean stress adjusted damage is also included; this will be detailed in **IV - 3**. Dye penetrant testing technique was used to analyse damaged shackles for the identification of fatigue cracks. Shackles 1-3 were left undamaged as a control for future tests.

Shackle	Test	Failure	No	Accumulated	Mean
4	Low	No	4,958	0.023	<i>0.127</i>
5	Low	No	4,958	0.023	<i>0.127</i>
6	Med	No	19,386	0.09	<i>0.456</i>
7	Med	No	19,386	0.09	<i>0.456</i>
8	Med	BREAK	19,386	0.09	<i>0.456</i>
9	High	Fatigue	24,344	0.113	<i>0.583</i>
10	High	Fatigue	24,344	0.113	<i>0.583</i>
11	High	BREAK	24,344	0.113	<i>0.583</i>

**Table 1: Fatigue test results including calculated accumulated damage based on S-N curve [15] for comparison, 1 equates to failure. Mean stress adjusted accumulated damage is included in italics; see IV-3 for further information.**

## IV DISCUSSION OF RESULTS

### IV - 1 FEA models

The

### IV - 2 Break loads

The break loads observed are significantly higher than the MBL specified by the manufacturer as is clearly shown in Figure 4. The break loads agree within 4% and the differences in the 0-50,000N region are likely to be due to differences in the 'bedding in' of the system. This occurred during pre-tests for Break 1, but no pre-tests were conducted for Break 2.

The

- The shackles can survive loads significantly higher than the ratings quoted by the manufacturer; both shackles survived beyond 200kN despite having a WLL of 24.5kN and an MBL of 122.6kN. The average safety factor is 8.6 on the WLL and 1.7 on the MBL.
- The shackles yield at a load slightly over 100kN, under the rated MBL.

### IV - 3 Fatigue tests

Failures and cracks occurred earlier than anticipated from the S-N curve which suggests a

p

**Figure 6.** The 10kN pre-tension applied throughout the fatigue testing regime creates a mean stress on the shackles. It is widely accepted that the presence of a mean stress during cyclical loading can significantly affect the fatigue life of a component. Whilst the S-N curve predicts lifetime for a fully reversed fatigue loading regime (a mean stress of 0), it is possible to use a mean stress adjustment factor to calculate an equivalent stress amplitude  $\sigma_{ar}$  to account for the presence of a mean stress,  $\sigma_m$ , which in this case is 75MPa. A review of the literature on this effect was conducted [21-24] and various mean stress adjustment factors were investigated. The most appropriate adjustment for general use appears to be the Smith, Watson and Topper (SWT) approach:

$$\sigma_{ar} = \sqrt{\sigma_{max}\sigma_a} \quad (9)$$

Where  $\sigma_{ar}$  is the equivalent stress amplitude for a completely reversed loading situation,  $\sigma_{max}$  is the maximum stress, and  $\sigma_a$  is the stress amplitude.

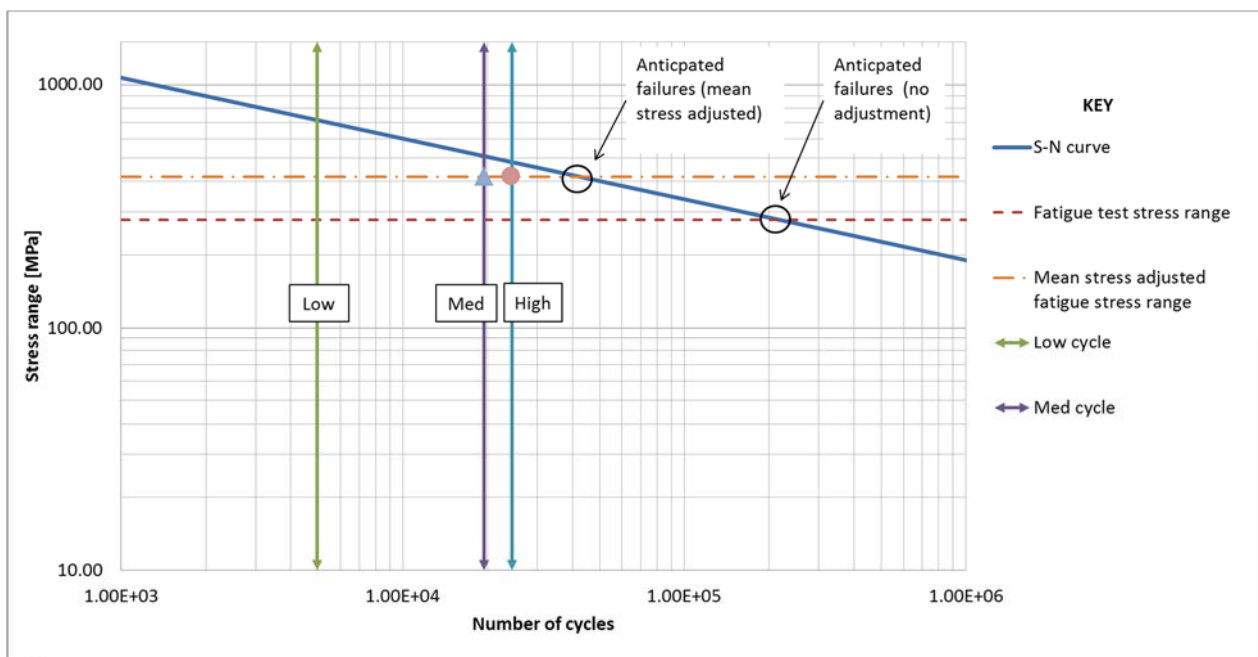


**Figure 6: S-N curve for shackles [15]. Fatigue test stress range and mean stress adjusted stress range identified, the difference between these being the acceleration level created by the**

u

r

e

,

s



presence of mean stress throughout the testing regime. Cycling regimes identified (low/med/high cycles, see Table 1). Failures plotted accounting for mean stress effects and identified by: ▲ denoting Shackle 8 break; ● denoting Shackle 11 break and Shackles 9 and 10 fatigue cracks.

This results in the mean stress adjusted accumulated damage figures detailed in

Shackle	Test	Failure	No	Accumulated	Mean
4	Low	No	4,958	0.023	0.127
5	Low	No	4,958	0.023	0.127
6	Med	No	19,386	0.09	0.456
7	Med	No	19,386	0.09	0.456
8	Med	BREAK	19,386	0.09	0.456
9	High	Fatigue	24,344	0.113	0.583
10	High	Fatigue	24,344	0.113	0.583
11	High	BREAK	24,344	0.113	0.583

$\bar{\sigma}$  is the equivalent stress amplitude for a completely reversed loading situation,  $\sigma_{max}$  is the maximum stress, and  $\sigma_a$  is the stress amplitude.

**Figure 6.** Accounting for the mean stress using this approach provides fatigue life estimations closer to the observed results.

Shackles 9 – 11 showed consistent behaviour, with a fatigue crack developing in the centre of the pin under tension, leading to complete failure in Shackle 11. The fatigue failure that occurred in the bow of Shackle 8 was a surprising failure due to the location as well as the low number of cycles. Repeat tests are required to draw sound conclusions, but this shackle may have had an inherent defect that led to this failure.

Under fatigue loading to 90kN, a safety factor of 3.7 on the WLL and 0.7 on the MBL are present.

## V SYNTHESIS, CONCLUSIONS AND FURTHER WORK

The FEA models accurately highlighted areas of weakness in the shackle. However, both the Break Tests and Fatigue Tests showed the shackles to be considerably stronger than estimated by the FEA models. The boundary conditions of the FEA models have affected these results, particularly in the pin model. Further models should be developed to refine these boundary conditions, and develop one model combining the interactions between the pin and the bow. Further to this, a model should be developed to investigate the effects of fatigue loading on the shackle.

The Break Tests confirmed the large safety factors present in the shackle specification, with the average failure load showing a safety factor of 8.6 on the shackle WLL. The Fatigue Tests showed that despite withstanding loads of over 200kN in the Break Tests, failures occurred with a load of 90kN when applied cyclically in the region of 20,000 cycles. This is a reduced safety factor of 3.7 on the WLL, below the MBL specified by the shackle supplier and earlier than the 215,000 cycles to failure anticipated from the S-N curve. Accounting for mean stress effects improves the agreement between test results and the S-N curve, and one would expect 42,000 cycles to failure, but this is still twice the observed test results. Further investigation into this is required; incorporating stress concentration factors with the use of the S-N curve as suggested by DNV [3] may further improve the agreement between the S-N curve and observed results.

The nature of WEC moorings dictates the components will be subject to fatigue loading, and pre-tension applied to mooring lines will frequently create mean stress loading situations. Component safety factors are not always specific to static or fatigue loading regimes, and specific S-N data is hard to obtain, so designers must rely on generic curves. DNV guidance to mooring designers [3] provides further safety factors that are more specific to the loading application. However, if the suggested

safety factor of 1.7 was applied to the break test results a total WLL safety factor of 14.6 would be present, and with a safety factor of 5 applied to the fatigue results a total WLL safety factor of 18.5 is present. Fatigue failure prediction is inherently burdened with scatter, so safety factors are necessary; however these results indicate safety factors may be excessive and creating unnecessary costs. If safety factors are to be reduced, the combined approach suggested here, culminating in service simulation testing of components to observed environmental loads is critical if we are to apply adequate but not excessive safety factors.

The experimental results presented in this paper are based on a small sample of shackles from one manufacturer. Good agreement is found between the results; however, a larger sample size is required to substantiate these findings. Additionally, in a saline environment the effects of corrosion on components should be considered when specifying safety factors and will be a continuation to this work.

## VI ACKNOWLEDGEMENTS AND THANKS

The authors would like to acknowledge the support of the UK Centre for Marine Energy Research (UKCMER) through the SuperGen programme funded by the Engineering and Physical Sciences Research Council. The authors would also like to thank David Parish for his valuable input, Andrew Vickers for his assistance with the DMaC, and David Raymond and Baptiste Chardon for their assistance with dye penetrant sample preparation.

## VII REFERENCES AND CITATIONS

- [1] Low Carbon Innovation Coordination Group (2012). - *Technology Innovation Needs Assessment (TINA) Marine Energy Summary Report*.
- [2] Carbon Trust (Black & Vetach) (2007). - *Key Marine Energy Component Technologies for Cost Reduction R&D*. Carbon Trust Website.
- [3] Det Norske Veritas (2010). - *Offshore Standard DNV-OS-E301 Position Mooring*. October.
- [4] Clément, A., et al. (2002). - *Wave energy in Europe: current status and perspectives*. Renewable and Sustainable Energy Reviews, **6**(5): p. 405-431.
- [5] Thorpe, T. (2010). - *2010 Survey of energy resources*. World Energy Council.
- [6] Wolfram, J. (2006). - *On assessing the reliability and availability of marine energy converters: the problems of a new technology*. Proceedings of the Institution of Mechanical Engineers, Part O: Journal of Risk and Reliability, **220**(1): p. 55-68.
- [7] Drew, B., A. Plummer, and M.N. Sahinkaya (2009). - *A review of wave energy converter technology*. Proceedings of the Institution of Mechanical Engineers, Part A: Journal of Power and Energy, **223**(8): p. 887-902.
- [8] RenewableUK (2011). - *Wave and tidal energy in the UK: State of the industry report*.
- [9] Arup, D.O. (2002). - *Sustainable energy technology route maps: Wave energy*.
- [10] Boud, R. (2002). - *Status and research and development priorities 2003. Wave and marine current energy*. UK Department of Trade & Industry.
- [11] Mueller, M. and H. Jeffrey (2008). - *UKERC marine (wave and tidal current) renewable energy technology roadmap*. in UK Energy Research Centre, University of Edinburgh. See [http://ukerc.rl.ac.uk/Roadmaps/Marine/Tech\\_roadmap\\_summary%20HJMWMM.pdf](http://ukerc.rl.ac.uk/Roadmaps/Marine/Tech_roadmap_summary%20HJMWMM.pdf).
- [12] DECC (2010). - *Marine energy action plan: Executive summary and recommendations*.
- [13] Thies, P.R., et al. (2013). - *Mooring line fatigue damage evaluation for floating marine energy converters: Field measurements and prediction*. Renewable Energy, under review. .
- [14] Harnois, V., L. Johanning, and P.R. Thies (2013). - *Wave Conditions Inducing Extreme Mooring Loads on a Dynamically Responding Moored Structure (draft)*. in EWTEC: Aalborg, Denmark.
- [15] Det Norske Veritas (2011). - *DNV-OS-C101: Fatigue design of offshore steel structures*. in DNV, Oslo, Norway.
- [16] (2013). - *Van Beest FTP server*. 2013 [cited September 2012]; Available from: [ftp://ftp.vanbeest.nl/Extra/GuestAZ/Out/Green Pin CAD Drawings V03/DWG files/](ftp://ftp.vanbeest.nl/Extra/GuestAZ/Out/Green_Pin_CAD_Drawings_V03/DWG_files/).

- [17] (2013). - *Dynamic Marine Component Test Facility (DMaC)*. 2013 [cited May 2013]; University of Exeter website description of DMaC capabilities. Available from: <http://emps.exeter.ac.uk/renewable-energy/research/research-interests/offshore/reliability/facilities/dynamicmarinecomponenttestfacilitydmac/>.
- [18] Carbon Trust (2005). - *Guidelines on the design and operation of wave energy converters*. Commissioned by the Carbon Trust and prepared by Det Norske Veritas.
- [19] Det Norske Veritas (2011). - *Fatigue design of offshore steel structures*. Recommended Practice DNV-RPC203.
- [20] (2011). - *ANSYS Mechanical Application User's Guide*. ANSYS. p. 1330.
- [21] Dowling, N., C. Calhoun, and A. Arcari (2009). - *Mean stress effects in stress-life fatigue and the Walker equation*. *Fatigue & Fracture of Engineering Materials & Structures*, **32**(3): p. 163-179.
- [22] Koh, S.K.S., R.I. (1991). - *Mean stress effects on low cycle fatigue for a high strength steel*. *Fatigue Fracture Engineering Materials and Structures*, **14**(4): p. 413-428.
- [23] Smith, K.N., T. Topper, and P. Watson (1970). - *A stress-strain function for the fatigue of metals (Stress-strain function for metal fatigue including mean stress effect)*. *Journal of Materials*, **5**: p. 767-778.
- [24] Wehner, T. and A. Fatemi (1991). - *Effects of mean stress on fatigue behaviour of a hardened carbon steel*. *International journal of fatigue*, **13**(3): p. 241-248.